VOL. 9, NO. 8, AUGUST 2014 ISSN 1819-6608
ARPN Journal of Engineering and Applied Sciences

www.arpnjournals.com

CREEP BEHAVIOR IN AN ANISOTROPY ROTATING DISC OF AL-SICW HAVING VARYING THICKNESS IN PRESENCE OF RESIDUAL STRESS

Vandana Gupta and S. B. Singh
Department of Mathematics, Punjabi University, Patiala, Punjab, India
E-Mail: vaggarwal2584@gmail.com

ABSTRACT

In the present study, the influence of anisotropy on the creep behavior of a rotating disc made of Al-SiCw composite having varying (linearly/non linearly) thickness has been studied in the presence of thermal residual stress. The steady state creep behavior is described by Sherby's creep law. The creep behavior has been analyzed using isotropic/anisotropic Hoffman yield criterion. The creep parameters have been evaluated using the available experimental results in the literature using regression analysis. The stress and strain rate distributions are calculated for different combinations of anisotropic constants. It is concluded that the effect of anisotropy in composite rotating disc with thermal residual stress has a significant change on strain rate, although, its effect on stresses is relatively small.

Keywords: anisotropic composites, rotating disc, creep, residual stress, strain rate.

1. INTRODUCTION

The Residual stresses exist within a body in the absence of external loading. Processing of the composites often involves cooling from higher temperature resulting in thermal residual stresses in the matrix due to restraint imposed by reinforcements. The magnitude of residual stresses can be investigated by determining the difference of yield stresses in tension and compression. Thermal residual stresses affect the mechanical properties of materials thereby shortening their lifetime. Residual stress significantly affects the engineering properties of materials and structural components, notably fatigue life, distortion, dimensional, corrosion resistance, brittle fracture etc. For that reason, the residual stress analysis is an important stage in the design of parts and structural elements. As a result, research on development of analytical models capable of performing plastic stress/strain analysis for rotating disc in presence of residual stresses, has become a necessity. Numbers of researchers (Wahl *et al*., 1954; Arya and Bhatnagar, 1979; Mishra and Pandey, 1990; Gupta *et al*., 2004; Baykara, 2007) have studied the creep behavior in a composite constant thickness disc reinforced of ceramic particles/whiskers into aluminum/aluminum alloy matrix at elevated temperature using different yield criteria and creeplaw. Nieh *et al*. (1984) has shown that an aluminum based composite containing silicon carbide particulate or whisker has better creep resistance compared to the base aluminum alloy which have isotropic mechanical properties convenient for design engineers.

Orcan and Eraslan (2002) investigated the stress distribution, displacement and plastic strain in a rotating elastic–plastic solid disc of variable thickness in a power function. The analysis is done on the basis of Tresca's yield criteria. He has noticed that by employing a variable thickness disc, the plastic limit angular velocity increases and the magnitude of stresses and deformations in the disc reduces. Jahed *et al*. (2005) observed that the use of variable thickness disc helps in minimizing the weight of disc which helps to reduce the overall payload in aerospace industry. This implies that a disc with variable thickness has no restrictions on the limiting value of maximum disc speed compare to a disc with constant thickness. Sayman *et al*. (2006) investigated elastic-plastic and residual stresses in thermoplastic composite laminated plates under linear thermal loading and also carried out an elastic-plastic, thermal stress analyses on thermoplastic composite disc reinforced with steel fibers under uniform temperature distribution and concluded that plastic yielding expands both around inner and outer surfaces and plastic flow is highest at the inner surface. Singh (2008) have studied creep behavior of a whisker reinforced anisotropic rotating disc with constant thickness. He described creep behavior by Norton's power law and concluded that anisotropy appears to help in restraining creep response both in the tangential and in the radial directions over the entire disc. Gupta *et al*. (2009) has investigated the effect of SiC morphology on the creep behavior of composite disc with constant thickness by Sherby's creep law and concluded that the creep stresses and creep rates are significantly affected by the morphology of SiC. Chamoli *et al*. (2010) have studied the effect of anisotropy on the stress and strain rates and concluded the anisotropy of the material has a significant effect on the creep of a rotating disc. The creep behavior is described by Sherby's law. Singh and Rattan (2010) has investigated the stress distributions and the resulting creep deformation in isotropic rotating disc having constant thickness and made of silicon carbide particulate reinforced aluminum base composite in presence of thermal residual stress. It is concluded that the presence of the tensile residual stress affects the distribution of stresses and strain in the disc with constant thickness. Vandana and Singh (2011) have studied the effect of anisotropy on the stress and strain rates in composite disc made of anisotropic material and concluded that the anisotropy of the material has a significant effect on the creep of a rotating disc with varying thickness. Steady state creep has been analyzed using the Sherby's constitutive model.

Keeping in view, an effort has been made to study creep response of a rotating composite disc with variations in the thickness (linear and hyperbolic) for isotropic/anisotropic material. The volume of all the discs is kept the same. Steady state creep has been analyzed using the Sherby's constitutive model. The disc is supposed to be made of composite containing silicon carbide whiskers (SiCw) embedded in a matrix of pure aluminum. The creep parameters have been evaluated using the available experimental results in the literature using regression analysis. The analysis has been done with thermal residual stresses.

2. MATHEMATICAL FORMULATION

Consider the particle reinforced composite disc of density ρ inner and with variable thickness h, rotating with constant angular speed ω radian/sec. a and b be inner and outer radii of the disc respectively. Let I and I_0 be the moment of inertia of the disc at inner radius a and outer radius r and b, respectively. A and A_0 be the area of cross section of disc at inner radius a and outer radius r and b respectively. Then,

$$I = \int_a^r h\, r^2 dr, \qquad I_0 = \int_a^b h\, r^2\, dr$$

$$A = \int_a^r h\, d\, r, \qquad A_0 = \int_a^b h\, dr \tag{1}$$

where, the average tangential stress may be defined as

$$\sigma_{\theta\, avg} = \frac{1}{A_0} \int_a^b h\, \sigma_\theta\, dr. \tag{2}$$

For the purpose of creep analysis in disc with variable thickness, the following assumptions are made:

a) Material of disc is orthotropic and incompressible
b) Elastic deformations are small for the disc and therefore they can be can be neglected as compared to creep deformation.
c) Axial stress in the disc may be assumed to be zero as thickness of disc is assumed to be very small compared to its diameter.
d) The composite shows a steady state creep behavior , which may be described by following Sherby's constitutive model (1977) of the form,

$$\dot{\bar{\varepsilon}} = A_s \left(\frac{\bar{\sigma} - \sigma_0}{E} \right)^n$$

where, $A_s = \dfrac{A D_\lambda \lambda^3}{|b_r|^5}$

where, $\dot{\bar{\varepsilon}}$, $\bar{\sigma}, n$, σ_0, A, D_λ, λ, b_r , E be the effective strain rate, effective stress, the stress exponent, threshold stress, a constant, lattice diffusivity, the sub grain size, the magnitude of burgers vector , Young's modulus.
The above equation may be expressed as,

$$\dot{\bar{\varepsilon}} = \left(M \left(\bar{\sigma} - \sigma_0 \right) \right)^n \tag{3}$$

where

$M = \dfrac{A_s^{1/n}}{E}$ is Creep Parameter.

The different material combinations in the composite are conceptually replaced by an equivalent monolithic material that has the yielding and creep behavior similar to those displayed by the composite. Taking reference frame along the principal directions of r, θ and z, the generalized constitutive equations for an anisotropic disc under multiaxial stress condition are given as,

$$\dot{\varepsilon}_r = \frac{\dot{\bar{\varepsilon}}}{2\bar{\sigma}} \left\{ (G+H)\sigma_r - H\sigma_\theta - G\sigma_z + (f_c - f_t) \right\} \tag{4}$$

$$\dot{\varepsilon}_\theta = \frac{\dot{\bar{\varepsilon}}}{2\bar{\sigma}} \left\{ (H+F)\sigma_\theta - F\sigma_z - H\sigma_r + (f_c - f_t) \right\} \tag{5}$$

$$\dot{\varepsilon}_z = \frac{\dot{\bar{\varepsilon}}}{2\bar{\sigma}} \left\{ (F+G)\sigma_z - G\sigma_r - F\sigma_\theta + (f_c - f_t) \right\} \tag{6}$$

where the effective stress, $\bar{\sigma}$, is given by

$$\bar{\sigma} = \left\{ \frac{1}{(G+H)} \left[F(\sigma_\theta - \sigma_z)^2 + G(\sigma_z - \sigma_r)^2 + H(\sigma_r - \sigma_\theta)^2 \right] \right\}^{1/2}$$

where F , G and H are anisotropic constants of the material. $\dot{\varepsilon}_r$, $\dot{\varepsilon}_\theta$, $\dot{\varepsilon}_z$ and σ_r , σ_θ , σ_z are the strain rates and the stresses respectively in the direction r, θ and z. $\dot{\bar{\varepsilon}}$ be the effective strain rate and $\bar{\sigma}$ be the effective stress and f_c , f_t are uniaxial compression and tensile yield stresses, respectively. For biaxial state of stress $(\sigma_r, \sigma_\theta)$, the effective stress is,

$$\bar{\sigma} = \left\{ \frac{1}{(G+H)} \left\{ F\,\sigma_\theta^2 + G\sigma_r^2 + H(\sigma_r - \sigma_\theta)^2 \right\} \right\}^{1/2} \tag{7}$$

Using Equations (3) and (7), Equation (4) can be rewritten as,

$$\dot{\varepsilon}_r = \frac{d\dot{u}_r}{dr} = \frac{\left[\left(\frac{G}{F}+\frac{H}{F}\right)x - \frac{H}{F} + \frac{f_c - f_t}{\sigma_\theta}\right]\left[M\left(\bar{\sigma}-\sigma_0\right)\right]^8}{\sqrt{\frac{G}{F}+\frac{H}{F}}\left[\left(\frac{G}{F}+\frac{H}{F}\right)x^2 - 2\frac{H}{F}x + \left(\frac{G}{F}+\frac{H}{F}\right)\right]^{1/2}} \tag{8}$$

Similarly from Equation (5),

$$\dot{\varepsilon}_\theta = \frac{\dot{u}_r}{r} = \frac{\left[\left(1+\frac{H}{F}\right) - \frac{H}{F}x + \frac{f_c - f_t}{\sigma_\theta}\right]\left[M\left(\bar{\sigma}-\sigma_0\right)\right]^8}{\sqrt{\frac{G}{F}+\frac{H}{F}}\left[\left(\frac{H}{F}+\frac{G}{F}\right)x^2 - 2\frac{H}{F}x + \left(1+\frac{H}{F}\right)\right]^{1/2}} \tag{9}$$

From the material's incompressibility assumption, it follows that

$$\dot{\varepsilon}_z = -\left(\dot{\varepsilon}_r + \dot{\varepsilon}_\theta\right) \tag{10}$$

where, $x = \frac{\sigma_r}{\sigma_\theta}$, is the ratio of radial and tangential stresses and $\dot{u}_r = du/dt$ is the radial deformation rate.

Dividing Eq. (7.1) by Eq. (7.2),

$$\phi(r) = \frac{\left((G/F)+(H/F)\right)x - (H/F) + ((f_c - f_t)/\sigma_\theta)}{\left(1+(H/F)\right) - (H/F)x + ((f_c - f_t)/\sigma_\theta)} \tag{11}$$

where

$$\phi(r) = \frac{d\dot{u}_r}{dr} \cdot \frac{r}{\dot{u}_r}$$

This implies,

$$\frac{d\dot{u}_r}{\dot{u}_r} = \frac{\phi(r)}{r}dr$$

Integrating and taking limit a to r on both sides,

$$\dot{u}_r = \dot{u}_{r_i} \exp\int_a^r \frac{\phi(r)}{r}dr \tag{12}$$

where, $\dot{u}_{r_i}$, is the radial deformation rate at the inner radius.

Dividing Equation (12) by r and equated to Equation (2),

$$\bar{\sigma} - \sigma_0 = \frac{(\dot{u}_{r_i})^{1/8}}{M}\psi(r) \tag{13}$$

where

$$\psi(r) = \left\{ \frac{\sqrt{\frac{G}{F}+\frac{H}{F}}}{r} \cdot \frac{\left[\left(\frac{H}{F}+\frac{G}{F}\right)x^2 - \frac{2Hx}{F} + \left(1+\frac{H}{F}\right)\right]^{1/2}}{\left[\left(1+\frac{H}{F}\right) - \frac{H}{F}x + \frac{f_c - f_t}{\sigma_\theta}\right]} \exp\int_a^r \frac{\varphi(r)dr}{r} \right\}^{1/8} \tag{14}$$

Substituting $\bar{\sigma}$ from Equation (7) to Equation (13), it gives,

$$\left\{\left(\frac{F}{G+F}\right)\left[\left(\frac{G}{F}+\frac{H}{F}\right)x^2 - 2\frac{H}{F}x + \left(\frac{H}{F}+1\right)\right]\right\}^{1/2}\sigma_\theta - \sigma_0 = \frac{\left(\dot{u}_{r_i}\right)^{1/8}}{M}\psi(r)$$

This implies,

$$\sigma_\theta = \frac{\left(\dot{u}_{r_i}\right)^{1/8}}{M}\psi_1(r) + \psi_2(r) \tag{15}$$

where

$$\psi_1(r) = \frac{\psi(r)}{\left\{\left(\frac{F}{G+H}\right)\left[\left(\frac{G}{F}+\frac{H}{F}\right)x^2 - 2\frac{H}{F}x + \left(1+\frac{H}{F}\right)\right]\right\}^{1/2}} \tag{16}$$

and

$$\psi_2(r) = \frac{\sigma_0}{\left\{\left(\frac{F}{G+H}\right)\left[\left(\frac{G}{F}+\frac{H}{F}\right)x^2 - 2\frac{H}{F}x + \left(1+\frac{H}{F}\right)\right]\right\}^{1/2}} \tag{17}$$

The equation of equilibrium for a rotating disc with varying thickness can be written as,

$$\frac{d}{dr}\left(r\, h\, \sigma_r\right) - h\sigma_\theta + \rho\omega^2 r^2 h = 0 \tag{18}$$

Integrating Equation (18) within limits a to b and using Equation (1) and Equation (2),

$$\sigma_{\theta_{avg}} = \frac{1}{A_0}\rho\omega^2 I_0 \tag{19}$$

Substituting σ_θ from Equation (15) into Equation (2),

$$\frac{\left(\dot{u}_{r_i}\right)^{1/8}}{M} = \frac{A_0\ \sigma_{\theta_{avg}} - \int_a^b \psi_2(r).\, hdr}{\int_a^b \psi_1(r).\, hdr} \tag{20}$$

Using Equation (19) and Equation (20), Equation (15) becomes,

$$\sigma_\theta = \frac{\psi_1(r)\left[\rho\omega^2 I_0 - \int_a^b \psi_2(r).\,hdr\right]}{\int_a^b \psi_1(r).hdr} + \psi_2(r) \quad (21)$$

Integrating Equation (18) within limits a to r and use Equation (1),

$$\sigma_r = \frac{1}{r.h}\left[\int_a^r \sigma_\theta .h\,dr - \rho\omega^2 I\right] \quad (22)$$

Thus, the tangential stress σ_θ and radial stress σ_r are determined by Equation (21) and Equation (22). Then strain rates $\dot{\varepsilon}_r, \dot{\varepsilon}_\theta$ and $\dot{\varepsilon}_z$ calculated from Equations (5), (6) and (7).

2.1. Discs with linearly varying thickness

The thickness (h) of the composite disc having linearly varying thickness is assumed to be of the form,

$$h = h_b + 2c\,(b - r) \quad (23)$$

where $c = \frac{(h_a - h_b)}{2(b-a)} = 0.002859$ is the slope of a disc and h_a and h_b are the disc thickness at the inner and outer radii, respectively.

Since the volume of disc having linearly varying thickness is assumed equal to the volume of constant thickness disc, therefore,

$$\int_a^b 2\pi\, r\, h\, dr = \pi(b^2 - a^2)\,t \quad (24)$$

Substituting the value of h from Equation (23) into Equation (24),

$$h_a = \frac{3(b+a)t - h_b(2b+a)}{(b+2a)} \quad (25)$$

Using expression, the Equation (1) becomes,

$$A = (r-a)\,[h_b + c\,(2b - r - a)] \quad (26)$$

$$A_0 = (b-a)\,[h_b + c\,(b-a)] \quad (27)$$

$$I = \frac{h_b}{3}(r^3 - a^3) + \frac{2cb}{3}(r^3 - a^3) - \frac{c}{2}(r^4 - a^4) \quad (28)$$

$$I_0 = \frac{h_b}{3}(b^3 - a^3) + \frac{2cb}{3}(b^3 - a^3) - \frac{c}{2}(b^4 - a^4) \quad (29)$$

2.2. Discs with hyperbolic varying thickness

The thickness (h) of the composite disc having hyperbolically varying thickness is assumed to be of the form,

$$h = c\,r^m \quad (30)$$

where $c = 31.26$ and $m = -0.74$ are constants.

Since the volume of disc having hyperbolically varying thickness is assumed equal to the volume of constant thickness disc, therefore,

$$c = \frac{(m+2)(b^2 - a^2)t}{2(b^{m+2} - a^{m+2})} \quad (31)$$

Using the expression for thickness, the Equation (1) becomes,

$$A = c\left(\frac{r^{m+1} - a^{m+1}}{m+1}\right) \quad (32)$$

$$A_0 = c\left(\frac{b^{m+1} - a^{m+1}}{m+1}\right) \quad (33)$$

$$I = c\left(\frac{r^{m+3} - a^{m+3}}{m+3}\right) \quad (34)$$

$$I_0 = c\left(\frac{b^{m+3} - a^{m+3}}{m+3}\right) \quad (35)$$

3. NUMERICAL COMPUTATIONS

The stress distribution and strain rates are evaluated for the rotating discs having linearly varying thickness described in section 2 by iterative numerical scheme of computation depicted in Figure-1. In the first iteration, it is assumed that $\sigma_\theta = \sigma_{\theta_{avg}}$ over the entire disc radii. Substituting $\sigma_{\theta_{avg}}$ for σ_θ in equation (22) the first approximation value of σ_r i.e. $[\sigma_r]_1$ is obtained. The first approximation of stress ratio i.e. $[x]_1$, is obtained by dividing $[\sigma_r]_1$ by σ_θ which can be substituted in equation (2.11) to calculate first approximation of $\phi(r)$ i.e. $[\phi(r)]_1$. Now one carries out the numerical integration of $[\phi(r)]_1$ from limits of a to r and uses this value in equation (14) to obtain first approximation of

VOL. 9, NO. 8, AUGUST 2014 ISSN 1819-6608
ARPN Journal of Engineering and Applied Sciences

www.arpnjournals.com

$\psi(r)$ i.e. $[\psi(r)]_1$. Using this $[\psi(r)]_1$ and σ_0 in equation (16) and (17) respectively, $[\psi_1(r)]_1$ and $[\psi_2(r)]_1$ are found, which are used in equation (15) to find second approximation of σ_θ i.e. $[\sigma_\theta]_2$. Using $[\sigma_\theta]_2$ for σ_θ in equation (22), second approximation of σ_r i.e. $[\sigma_r]_2$ is found and then the second approximation of x i.e. $[x]_2$ is obtained. The iteration is continued till the process converges and gives the values of stresses at different points of the radius grid. For rapid convergence 75 percent of the value of σ_θ obtained in the current iteration has been mixed with 25 percent of the value of σ_θ obtained in the last iteration for use in the next iteration i.e. $\sigma_{\theta next} = .25\sigma_{\theta previous} + .75\sigma_{\theta current}$.

4. RESULTS AND DISCUSSIONS

A computer program based on the analysis presented in this article has been developed to investigate the effect of anisotropic constants i.e. $(G/F, H/F)$ in the composite varying thickness discs with residual stresses and obtained results are compared to the constant thickness disc with residual stresses. For the analysis, the tensile residual stress $(\Delta\sigma_y)$ is taken as 32MPa (used by Badini, 1990; Singh and Rattan, 2010).

Table-1. Anisotropic constants.

	Case-1	Case-2	Case-3	Case-4	Case-5
G/F	.8159	1.200	1.000	.7452	1.34
H/F	.6081	.7452	1.000	1.2200	1.64

For the sake of computation of a rotating disc made of silicon carbide particles (SiCp) reinforced in a matrix of pure aluminum matrix composite in presence of residual stresses, the anisotropic constants shown in Table-1, have been taken as in Chamoli *et al*. (2010) and the numerical results have been calculated for two cases of anisotropy each deviating from isotropy. The remaining two cases of anisotropy are almost similar and hence they have been omitted for computational purpose.

In Figure-1, the variation of tangential stress along the radius in the disc for two different cases of anisotropy has been investigated and the results are compared with an isotropic disc.

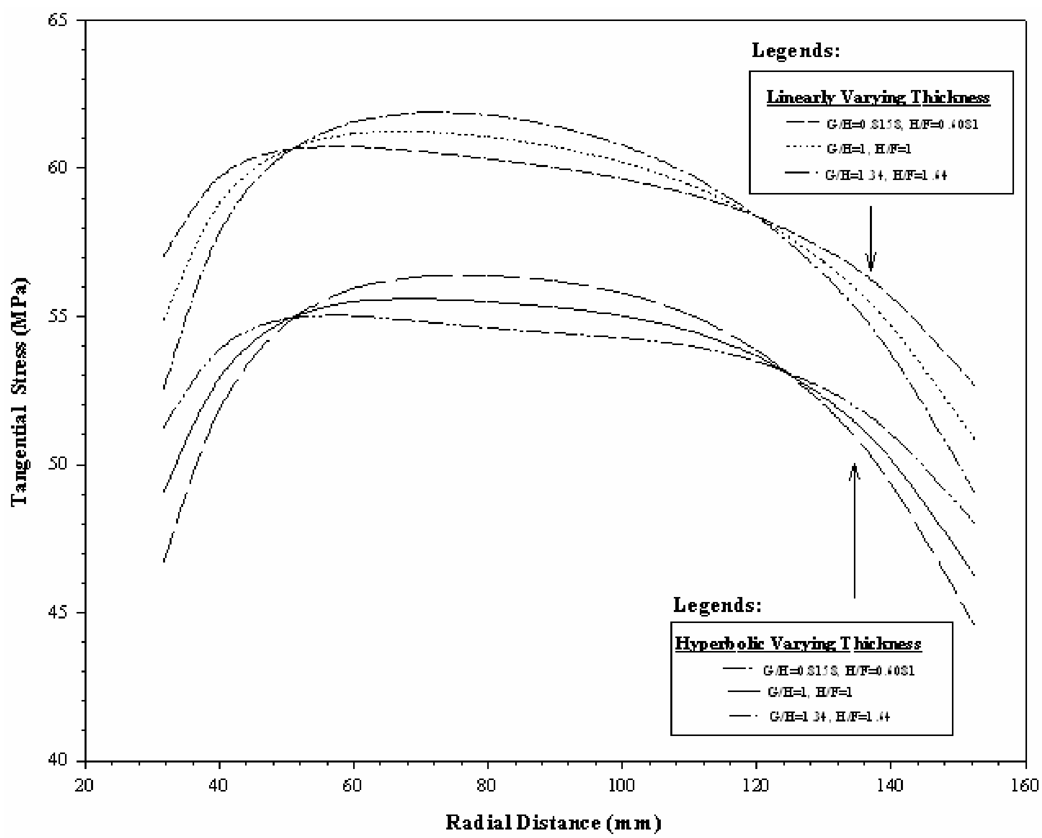

Figure-1. Variation of tangential stress along the radial distance of the isotropic/anisotropic discs in presence of residual stress rotating with an angular velocity 15000 rpm at 616K.

In presence of residual stress, if anisotropic constants i.e. $(G/F, H/F)$ are less than unity, the tangential stress enhances in inner and outer region of the disc in comparison to that in isotropic case, but reduces in middle part of disc. If anisotropic constants i.e. $(G/F, H/F)$ are greater than unity, the tangential stress reduce in the inner and outer region of the disc in comparison to that in isotropic case, but enhances in middle part of disc. The trend of variation of tangential stress is similar in all cases of thickness profile variations. It is concluded that effect of anisotropy is same on tangential stress in both thickness profile, although magnitude of effect is lesser in case of hyperbolically varying thickness.

Table-2. Parameters and operating conditions for steel disc.

Parameters for steel disc
Density of disc material $\rho = 2812.4\,kg/m^3$
Inner radius of disc, $a = 31.75mm$
Outer radius of disc, $b = 152.4mm$
Particle size, $P = 1.7\,\mu m$
Particle content, $V = 20\%$
Creep parameters for whisker reinforced disc, $M = 80.0 \times 10^{-4}\, s^{-1/8}/MPa$ and $\sigma_0 = 35.00\,MPa$
Young's modulus, $Al = 70\,GPa$
Young's modulus, $SiC = 47GPa$
Density, $Al = 2713\,kg/m^3$
Density, $SiC = 3210\,kg/m^3$
The stress exponent of disc, $n = 8$
The disc thickness for linearly varying thickness at the inner radii, $h_a = 1.44mm$
The disc thickness for linearly varying thickness at the outer radii, $h_b = 0.75mm$
The disc thickness for hyperbolically varying thickness at the inner radii, $h_a = 2.42mm$
The disc thickness for hyperbolically varying thickness at the outer radii, $h_b = 0.76mm$
Operating conditions
Angular velocity of Disc, $\omega = 15{,}000\,rpm$
Operating temperature, $T = 616\,K$
Creep duration, $t = 180\,hrs$

In Figure-2, the variation of radial stress along the radius in the disc for two different cases of anisotropy has been investigated and the results are compared with an isotropic disc. The values of radial stress are highest for $(G/F > 1, H/F > 1)$ and lowest for $(G/F < 1, H/F < 1)$ but the values for isotropic case $(G/F = 1, H/F = 1)$ lie between the two. It is evident that the change in the magnitude of radial stress distribution is very small due to introducing anisotropy in the disc with residual stress as compare to isotropic disc.

In Figure-3, the tangential strain rate is maximum for anisotropic constants i.e. $(G/F, H/F)$ greater than unity and minimum for anisotropic constants $(G/F, H/F)$ less than unity in comparison to that in isotropic case $(G/F = 1, H/F = 1)$. However, in all cases of thickness profile variation, the trend of variation of tensile strain rate in tangential direction remains the same, but the magnitude is reduced in disc with anisotropic constants $(G/F > 1, H/F > 1)$. Thus by choosing anisotropic constants i.e. $(G/F, H/F)$ greater than unity with hyperbolic varying thickness, the magnitude of effect of residual stress on tangential strain rate can be reduced.

In Figure-4, the variation of tangential stress along the radius in the disc for two different cases of anisotropy has been investigated and the results are compared with an isotropic disc. The magnitude of radial strain rate decreases with radial distance, reaches a minimum before increasing again towards the outer radius in every case of anisotropy and thickness profile. By reinforcing whisker in 6061Al matrix, it can be concluded that in presence of residual stress, the nature of radial strain rate which is compressive for

VOL. 9, NO. 8, AUGUST 2014 ISSN 1819-6608
ARPN Journal of Engineering and Applied Sciences

www.arpnjournals.com

$(G/F = 1,\ H/F = 1)$ and $(G/F > 1,\ H/F > 1)$, becomes tensile at the middle region of the disc for $(G/F < 1,\ H/F < 1)$. This change in strain distribution due to the anisotropy in the disc with varying thickness may cause unwanted deformation in shape. By selecting $(G/F > 1,\ H/F > 1)$ with hyperbolic variation in the disc with residual stress, the magnitude of radial strain rate can be reduced as compared to disc having linear variation.

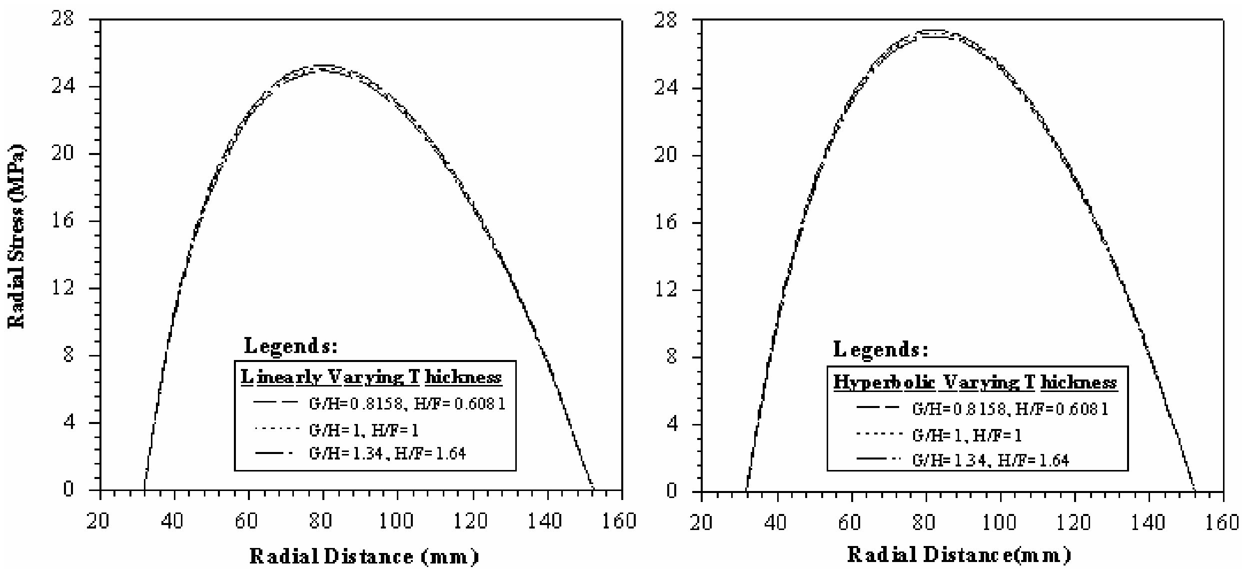

Figure-2. Variation of radial Stress along the radial distance of the isotropic/anisotropic discs in presence of residual stress rotating with an angular velocity 15000 rpm at 616K.

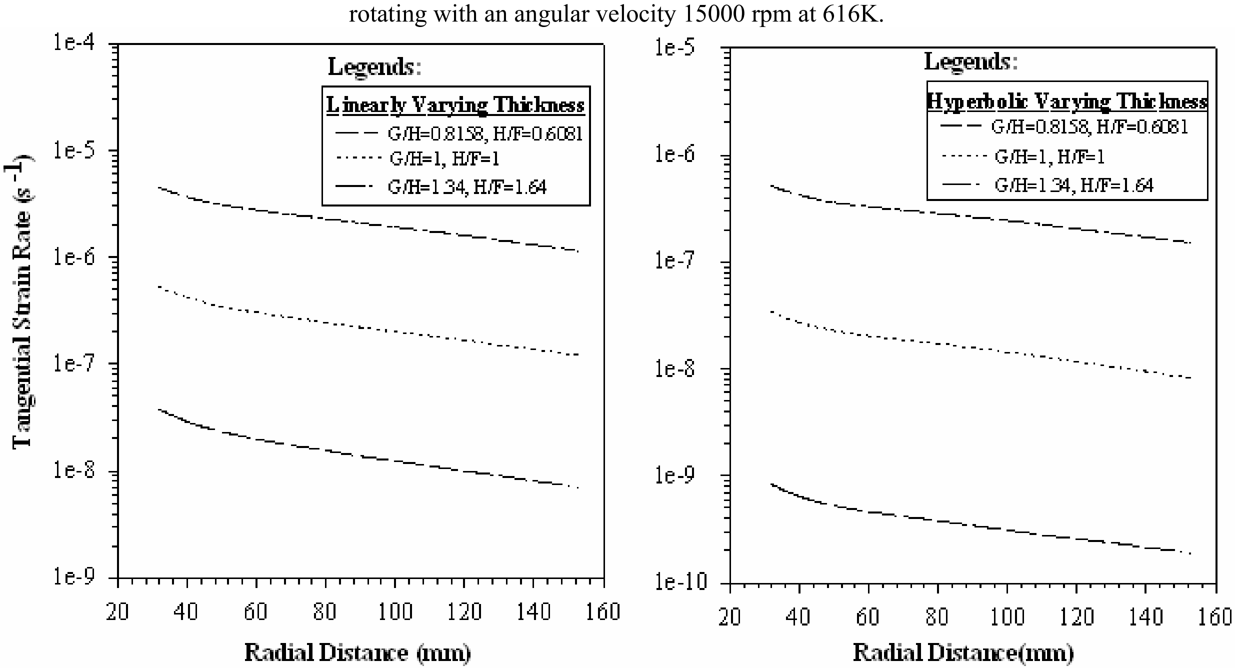

Figure-3. Variation of tangential strain rate along the radial distance of the isotropic/anisotropic discs in presence of residual stress rotating with an angular velocity 15000 rpm at 616K.

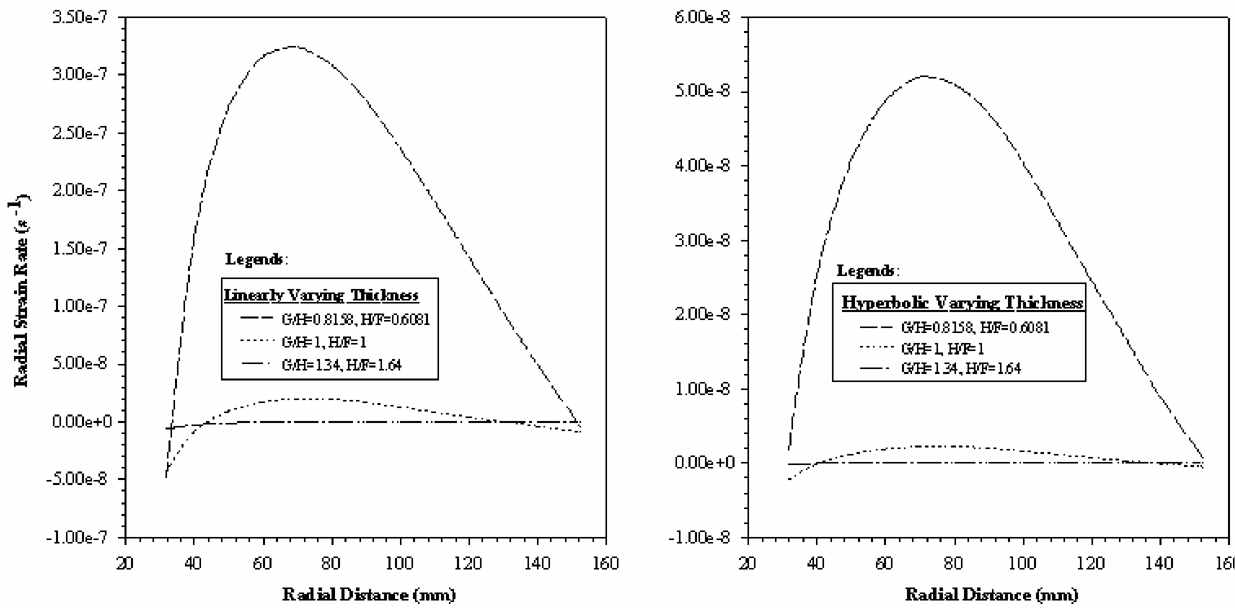

Figure-4. Variation of radial strain rate along the radial distance of the isotropic/anisotropic discs in presence of residual stress rotating with an angular velocity 15000 rpm at 616K.

CONCLUSIONS

The above results and discussion concludes that

a) The anisotropy of material significantly affects the strain rates in rotating composite disc having thermal residual stress, although its effect on the stresses distribution may be relatively small.

b) The trend of variation of tensile strain rate in tangential direction remains the same in discs with varying thickness, but by taking anisotropic constants i.e. $(G/F > 1,\ H/F > 1)$ with hyperbolically varying thickness in rotating composite disc having residual stress, the magnitude of tangential strain rate can be reduced by about three order of magnitude compared to those for isotropic composites with linearly varying thickness.

c) In a rotating disc having residual stress, the nature of the radial strain rate does is compressive for anisotropic constants i.e. $(G/F > 1,\ H/F > 1)$ in both the cases of thickness, but the magnitude of radial strain rate can be reduced by taking hyperbolic profile as compare to linear variation of thickness.

d) For designing a rotating composite disc in the presence of residual stress, the care should be taken to introduce anisotropy from the point of view of steady state creep.

REFERENCES

A.M. Wahl, G.O. Sankey, M.J. Manjoine and E. Shoemaker. 1954. Creep tests of rotating risks at elevated temperature and comparison with theory. Journal of Applied Mechanics. 76: 225-235.

O.D. Sherby, R.H. Klundt and A.K. Miller. 1977. Flow stress, subgrain size and subgrain stability at elevated temperature. Metallurgical Transactions A. 8(6): 843-850.

V.K. Arya and N.S. Bhatnagar. 1979. Creep analysis of rotating orthotropic disc. Nuclear Engineering and Design. 55: 323-330.

T.G. Nieh. 1984. Creep rupture of a silicon carbide reinforced aluminum composite. Metallurgical Transactions. 15A, 139-146.

P.S. Kulkarni, N.S. Bhatnagar and V.K. Arya. 1985. Creep analysis of thin-walled anisotropic cylinders subjected to internal pressure, bending and twisting. Proceedings of the workshop on solid mechanics. pp. 13-16.

J. Bialkiewicz. 1986. Dynamic creep rupture of a rotating disc of variable thickness. International Journal of Mechenical Science. 28(10): 671-681.

N.S. Bhatnagar, P.S. Kulkarni and V.K. Arya. 1986. Steady state creep of orthotropic rotating discs of variable thickness. Nuclear Engineering and Design. 91: 121-141.

C. Badini. 1990. SiC whiskers-aluminium 6061 composite: Mi-crostructure and mechanical characteristic anisotropy. Journal of Material Science. 25: 2607-2614.

R. S. Mishra and A. B. Pandey. 1990. Some observations on the high-temperature creep behaviour of 6061 Al-SiC composites. Metallurgical Transactions. 21A(7): 2089-2090.

A.B. Pandey, R.S. Mishra and Y.R. Mahajan. 1992. Steady state creep behavior of silicon carbide particulate reinforced aluminum composites. Acta Metallurgica Materialia. 40(8): 2045-2052.

Y. Orcan and A.N. Eraslan. 2002. Elastic-plastic stresses in linearly hardening rotating solid discs of variable thickness. Mechanics Research Communications. 29(4): 269-281.
S.B. Singh and S. Ray. 2002. Modeling the anisotropy and creep in orthotropic Al-SiC composite rotating disc. Mechanics of Materials. 34: 363-372.

V.K. Gupta. 2004. Steady state creep and material parameters in a rotating disc of Al-SiCp composite. European Journal of Mechanics A/Solids. 23: 335-344.

H. Jahed, B. Farshi and J. Bidabadi. 2005. Minimum weight design of inhomogeneous rotating discs. International Journal of Pressure Vessels and Piping. 82(1): 35-41.

O. Sayman. 2006. Stress analysis of a thermoplastic composite disc under uniform temperature distribution. Journal of Thermoplastic Composite Materials. 19: 61-77.

C. Baykara. 2007. Comparison of stress concentrations in thin sheets with plastic anisotropy. Journal of Reinforced Plastics and Composites. 26: 1455-1459.

S.B. Singh. 2008. One parameter model for creep in a whisker reinforced anisotropic rotating disc of Al-SiCw composite. European Journal of Mechanics A/Solids. 27(4): 680-690.

V.K. Gupta, S.B. Singh and S. Ray. 2009. Role of reinforcement geometry on the steady state creep behavior of a rotating composite disc. Multidiscipline Modeling in Materials and Structures. 5: 139-150.

N. Chamoli, M. Rattan and S.B. Singh. 2010. Effect of anisotropy on the creep of a rotating disc of Al-SiCp composite. Indian Journal of Contemporary Mathematical Sciences. 5(11): 509-516.

S.B. Singh and M. Rattan. 2010. Creep analysis of an isotropic rotating disc in the presence of thermal residual stress. Journal of Thermoplastic Composite Materials. 23: 299-312.

V. Gupta and S.B. Singh. 2011. Modeling anisotropy and steady state creep in a rotating disc of al-sicp having varying thickness. International Journal of Scientific and Engineering Research. 2(10): 1-12.